

Four-Wave Mixing with Short Temporally Nonoverlapping Pulses

A. D. Wilson-Gordon^{*,†} and H. Friedmann

Department of Chemistry, Bar-Ilan University, Ramat Gan 52900, Israel

Received: June 3, 1998; In Final Form: September 14, 1998

We predict that the four-wave mixing (FWM) excitation spectrum for a two-level system becomes extremely asymmetrical when steady-state excitation is replaced by pulsed excitation, using temporally nonoverlapping probe and pump pulses. We also show that when a resonant probe pulse precedes the detuned pump pulse, the FWM signal may become more intense than when the pulses overlap. These effects are attributed to free-induction decay (FID): the coherence induced in the two-level system by a short resonant probe pulse survives the pulse (FID) and replaces it in producing a strong nonlinear signal on interaction with the strong pump pulse. Moreover, by plotting the FWM signal intensity as a function of the delay between the probe and pump pulses, an efficient method is proposed for determining short transverse relaxation times or fast chemical reaction rates.

1. Introduction

The steady-state excitation four-wave mixing (FWM) spectrum obtained when a two-level system interacts with a monochromatic coherent pump of arbitrary intensity and fixed frequency, ω_1 , and a weak monochromatic coherent probe of varying frequency, ω_2 , has been studied in detail by Boyd and co-workers.¹ A symmetrical three-peaked spectrum is obtained with the central peak at $\delta = \omega_2 - \omega_1 = 0$ and two Rabi sidebands at $\delta = \pm\Omega_1$, where the generalized pump Rabi frequency, $\Omega_1 = (\Delta_1^2 + 4|V_1|^2)^{1/2}$, is determined by the pump detuning from resonance, $\Delta_1 = \omega_{ba} - \omega_1$, and Rabi frequency, $2V_1 = \mu E_1/\hbar$. In the limit of large detuning, $\Delta_1 \gg 2|V_1|$, one of the peaks is situated near the resonance frequency, $\omega_2 \approx \omega_{ba}$, and the other near the three-photon scattering (TPS), or hyper-Raman, frequency, $\omega_2 \approx 2\omega_1 - \omega_{ba}$.

When pulsed pump and probe fields are used, FWM spectra which differ considerably from the steady-state theoretical predictions are obtained.² The interaction of coherent pulses with a two-level system is the most fundamental problem in nonlinear optics³ and forms the basis for understanding the interaction of pulses with multilevel systems. Thus, a time-dependent generalization of the theory of Boyd *et al.*¹ is required. In a previous publication² we presented such a generalization and discussed the case of overlapping pulses for which experimental evidence is available.²

In this paper, we will show that a completely different picture emerges when the FWM is obtained with temporally nonoverlapping pump and probe pulses. The excitation spectrum becomes extremely asymmetrical and only the Rabi sideband near the resonance frequency survives, in the case where the probe pulse precedes the pump pulse. In the opposite case where the probe follows the pump, no FWM spectrum is obtained at all. It should be noted that these results hold provided the pump and probe durations, D_1 and D_3 , are much shorter than the transverse relaxation time, T_2 , and also shorter than the time delay between the pump and probe, Δt_0 . We will also compare the intensity of the Rabi sideband at the resonance frequency for the case where the temporally nonoverlapping

resonant probe precedes the pump pulse with that where the pulses overlap. The surprising result is that the nonoverlapping pulses may yield a stronger spectrum than the overlapping pulses. The crucial point is that the pump need not overlap with the probe itself but rather with the atomic system's *coherent response to the probe* that only reaches its maximum value when the probe pulse is nearly finished, and then decays by free induction decay (FID)³ at a rate proportional to $1/T_2$. Since our theory is nonperturbative in the pump field, we shall be able to show that FID on interaction with a strong pump pulse produces strong nonlinear optical (FWM) signals. In addition, we shall show that it is possible to determine the value of T_2 from the slope of the semilog plot of the FWM intensity versus the pump–probe delay time, even for quite intense pump pulses that give correspondingly strong FWM signals.

It should be noted that T_2 is used as a scaling factor in all our calculations. Thus, for example, the Rabi frequency is written in dimensionless units as $2VT_2$. The practical implication of this is that in order to obtain the same signal strength when T_2 is in the picosecond regime as when it is in the nanosecond regime, one will require the value of V to be 3 orders of magnitude greater. As will be discussed in section 3, nonperturbative, nondegenerate FWM is particularly suited to measuring ultrashort values (of the order of picoseconds or shorter) of T_2 , which in the case of reactive collisions corresponds to the inverse reaction rate.

Delayed pulse techniques have also been studied in pulsed four-wave mixing² and in the coherent population transfer technique called stimulated Raman adiabatic passage (STIRAP) in three-level systems.^{4–12} The comparison between nonlinear optical effects such as STIRAP and pulsed FWM is particularly instructive. STIRAP requires some overlap between the pulses used to excite the one-photon transitions since usually these pulses are detuned from resonance. Thus the coherent response of the system does not survive either of the incident pulses. This is similar to pulsed FWM when the probe is at the (nonresonant) TPS sideband since then both fields are nonresonant. However, when the probe is at the resonance frequency, FID survives after the probe is switched off and replaces the pulse in the FWM process. This explains the predicted

[†] E-mail: gordon@mail.biu.ac.il.

asymmetry of the FWM spectrum when temporally nonoverlapping pulses are used. Note that if (at least) one of the exciting pulses in a Λ -three-level system is resonant with the transition it excites, then our theory, according to which the pulses can be replaced by the decaying matrix elements induced by it, applies. We then predict coherent population transfer provided short nonoverlapping $(2n + 1)\pi$ pulses are applied in the intuitive pulse order. We can then determine T_1 from the slope of a semilog plot of the population in the final level versus the delay between the pulses.

2. Theory

In a previous paper,² we used the Bloch equations for the interaction of a strong pulse, $E_1(t)$ and a weak probe, $E_2(t)$ to derive the equations of motion of the Fourier components of the density matrix to first order in $E_2(t)$ and to all orders in $E_1(t)$

$$i\dot{\rho}_{ab}(-\omega_1) = -(\Delta_1 + i/T_2)\rho_{ab}(-\omega_1) - V_1^*(t)(\rho_{bb} - \rho_{aa})^0 \quad (1)$$

$$(\dot{\rho}_{bb} - \dot{\rho}_{aa})^0 = -4\text{Im}[V_1(t)\rho_{ab}(-\omega_1)] - (1/T_1)(\rho_{bb} - \rho_{aa})^0 - 1/T_1 \quad (2)$$

$$i\dot{\rho}_{ba}(\omega_2) = (\Delta_1 - \delta - i/T_2)\rho_{ba}(\omega_2) + V_1(t)(\rho_{bb} - \rho_{aa})^{(\delta)} + V_2(t)(\rho_{bb} - \rho_{aa})^0 \quad (3)$$

$$i\dot{\rho}_{ab}(\omega_2 - 2\omega_1) = -(\Delta_1 + \delta + i/T_2)\rho_{ab}(\omega_2 - 2\omega_1) - V_1^*(t)(\rho_{bb} - \rho_{aa})^{(\delta)} \quad (4)$$

$$i(\dot{\rho}_{bb} - \dot{\rho}_{aa})^{(\delta)} = -(\delta + i/T_1)(\rho_{bb} - \rho_{aa})^{(\delta)} + 2V_1^*(t)\rho_{ba}(\omega_2) - 2V_1(t)\rho_{ab}(\omega_2 - 2\omega_1) - 2V_2(t)\rho_{ab}(-\omega_1) \quad (5)$$

Since the Rabi frequencies, $V_1(t)$ and $V_2(t)$, are time dependent, the Bloch equations of eqs 1–5 must be solved numerically. This allows us to calculate $|\rho_{ab}(\omega_2 - 2\omega_1)|^2$, which is proportional to the FWM intensity in the thin-slab approximation, as a function of the pump–probe detuning, δ , and time. In order to emphasize the physical origin of the phenomena, we shall not include propagation effects beyond the thin-slab approximation.

In order to compare the FWM signal obtained with pulses to that obtained using CW lasers in the steady state, we integrate $|\rho_{ab}(\omega_2 - 2\omega_1)|^2$ over time:

$$\langle |\rho_{ab}(\omega_2 - 2\omega_1)|^2 \rangle = \int_{-\infty}^{+\infty} |\rho_{ab}(\omega_2 - 2\omega_1)|^2 d(t/T_2) \quad (6)$$

where, in order to obtain a dimensionless quantity, T_2 is used as the unit of time.

The Bloch equations are solved for Gaussian-shaped pump and probe pulses:

$$V_1(t) = V_1 \exp(-t^2/D_1^2), \quad V_2(t) = V_2 \exp[-(t - \Delta t_0)^2/D_2^2] \quad (7)$$

where Δt_0 is the pump–probe delay time and the maximum pump Rabi frequency V_1 is much larger than the maximum probe Rabi frequency V_2 .

3. Results and Discussion

In Figure 1 we plot the FWM spectrum, calculated from eqs 1–7, for short ($D_1 = D_2 = 0.1T_2$), moderately weak ($V_1T_2 = 0.1$) pump pulse and weak probe pulse ($V_2T_2 = 0.001$), where

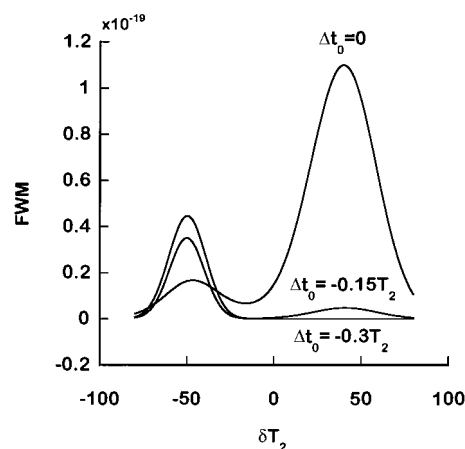


Figure 1. FWM spectrum as a function of pump–probe detuning, δT_2 , calculated from eqs 1–6, for short ($D_1 = D_2 = 0.1T_2$), moderately weak ($V_1T_2 = 0.1$), detuned ($\Delta_1T_2 = -50$) pump pulse and weak probe pulse ($V_2T_2 = 0.001$), for various values of the pump–probe delay, Δt_0 .

the pump is detuned from resonance ($\Delta_1T_2 = -50$). We compare the case where the pulses coincide ($\Delta t_0 = 0$) with those where the probe precedes the pump pulse ($\Delta t_0 = -0.15T_2, -0.3T_2$). For the case of simultaneous pulses, the Rabi sideband near the resonance frequency ($\delta T_2 = -50$) is weaker and narrower than that near the TPS frequency ($\delta T_2 = 50$). This asymmetry was discussed by us previously² and is a consequence of the poor overlap of the probe spectral line width with that of the atomic transition, which determines the resonance Rabi sideband, compared with its complete overlap with that of the pump which determines the TPS Rabi sideband. We see from Figure 1 that the intensity of the TPS sideband decreases rapidly as the pump–probe delay increases. We have also shown² that this intensity is a symmetrical function of the pump–probe delay.

The situation is quite different for the resonance sideband: here, the intensity is greatest (exceeding that obtained for simultaneous pulses) for $\Delta t_0 = -0.15T_2$, and decreases slowly as the pump–probe delay increases. Only for $\Delta t_0 \approx -0.6T_2$ does the intensity become equal to that obtained using simultaneous pulses. In addition, we have found that, in contrast to the TPS sideband, the intensity of the resonance sideband is a highly asymmetric function of the delay. When the probe follows the pump, the intensity decreases rapidly as the delay increases. For example, the intensity of the resonance sideband is 2 orders of magnitude smaller for $\Delta t_0 = 0.15T_2$ than for $\Delta t_0 = -0.15T_2$, and 7 orders of magnitude smaller for $\Delta t_0 = 0.3T_2$ than for $\Delta t_0 = -0.3T_2$.

The dramatic difference in behavior between the case where the probe precedes the pump and that where it follows the pump can be understood by considering Figure 2. Here, we plot $\text{Im}\rho_{ba}(\omega_2)$ as a function of time for a resonant probe ($\delta T_2 = \Delta_1T_2 = -50$) and various values of the pump–probe time delay. The Fourier component of the off-diagonal density matrix element at ω_2 , $\rho_{ba}(\omega_2)$, is the coherent response of the two-level system induced by the probe. The real part of $\rho_{ba}(\omega_2)$ is negligible compared to the imaginary part due to the fact that the probe is resonant. It should be noted that the coherent response is unmodified by the presence of the pump since the pump has been taken to be both relatively weak and far from resonance. Figure 2 shows that the maximum value of $\rho_{ba}(\omega_2)$ occurs at a time that is approximately $0.15T_2$ after the probe Rabi frequency reaches its maximum value at $t = \Delta t_0$. It then decreases due to FID. Thus, only if the pump follows the probe

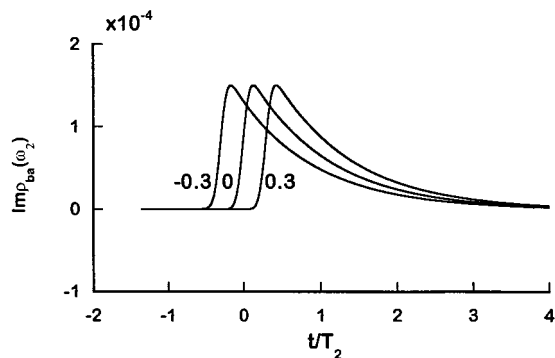


Figure 2. Time dependence of the atomic response $\text{Imp}_{ba}(\omega_2)$ to a resonant probe, for the same parameters as in Figure 1 with $\delta T_2 = -50$, and for various values of the pump-probe time delay, Δt_0 .

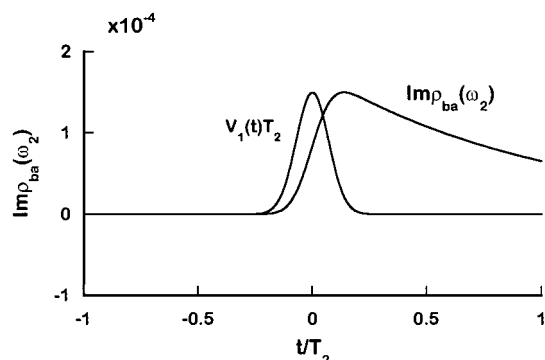


Figure 3. Time dependence of the atomic response $\text{Imp}_{ba}(\omega_2)$ to a resonant probe, for the same parameters as in Figure 2 for the case of overlapping pump and probe pulses, together with the dimensionless pump profile, $V_1(t)T_2$, normalized to the same height.

will it experience significant overlap with the FID tail, with maximum overlap occurring at $\Delta t_0 = -0.15T_2$. In order to emphasize the incomplete overlap between the pump and the coherent response of the atomic system to the probe for the case of overlapping pump and probe pulses, we plot $\rho_{ba}(\omega_2)$ and the pump profile (normalized to the same height) in Figure 3. The importance of the overlap between $\rho_{ba}(\omega_2)$ and the pump in determining the intensity of the resonance Rabi sideband explains both its asymmetry with respect to the pump-probe time delay and the fact that its maximum intensity is obtained for $\Delta t_0 = -0.15T_2$.

It should be noted that when the probe is at the TPS frequency, the coherent response follows the probe pulse adiabatically¹³ due to the large detuning of the probe from resonance. There is thus no FID tail that can overlap with a temporally delayed pump pulse and lead to a FWM signal. This explains the lack of symmetry between the Rabi sidebands in the FWM spectrum for temporally nonoverlapping pulses (see Figure 1).

In Figure 4, we plot the log of the time-integrated FWM, $\langle |\rho_{ab}(\omega_2 - 2\omega_1)|^2 \rangle$, at the resonance sideband as a function of the pump-probe delay, $\Delta t_0/T_2$, for various values of the pump Rabi frequency, for nonoverlapping pulses, with the probe preceding the pump. We see that the time-integrated FWM intensity increases strongly with the pump Rabi frequency. We also see that, even for fairly saturating pumps, a straight line of slope 2/2.303 is obtained or, alternatively,

$$-\frac{d \ln \langle |\rho_{ab}(\omega_2 - 2\omega_1)|^2 \rangle}{d\Delta t_0} = 2/T_2 \quad (8)$$

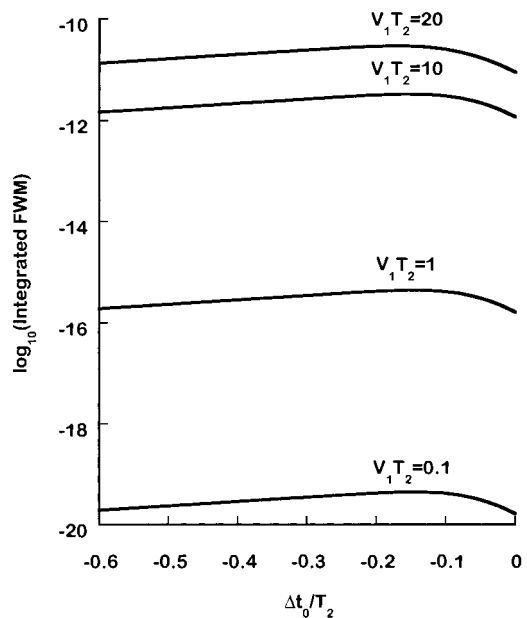


Figure 4. A logarithmic plot of the integrated FWM as a function of the pump-probe time delay, $\Delta t_0/T_2$, where the probe precedes the pump pulse, for various values of the maximum pump Rabi frequency, $V_1 T_2$. The parameters used are $\Delta_1 T_2 = -50$, $\delta T_2 = -50$, and $V_2 T_2 = 0.001$. In each case, for $\Delta t_0/T_2 < -0.2$ the slope is 2/2.303.

In conclusion, we have shown that nonoverlapping probe and pump pulses interacting with a two-level system reduce the steady-state symmetrical three-peaked FWM excitation spectrum to a single peak at the resonance Rabi sideband. Since FWM only occurs when the resonant probe pulse precedes the near-resonant pump pulse, we conclude that the effect is due to the overlap between the off-diagonal density-matrix element $\rho_{ab}(\omega_2)$ which decays at the rate $1/T_2$ (FID) and the pump pulse. Thus, FWM can be used as a tool for monitoring the complex FID tails obtained when strong short pulses interact with two-level atoms.¹⁴⁻¹⁷ We have shown that by varying the pump-probe delay, pulsed FWM becomes a tool for measuring T_2 , provided the pulses are shorter than T_2 . However, in the case of ultrashort relaxation times (of the order of picoseconds), the even shorter pulses (of the order of femtoseconds) would yield FWM signals which are too weak to be measured accurately unless their intensity is increased by using strong pump pulses. For such applications, our approach is particularly convenient since it is nonperturbative and valid to all orders in the pump intensity. Moreover, since we propose the use of nondegenerate FWM, the weak output signal is far from resonance and will not be absorbed by the medium. Our approach can also be used for monitoring ultrafast chemical reactions, where T_2 is a measure of the reaction rate. However, in order to distinguish between reactive and dephasing collisions, it is necessary to repeat the pump-probe pulse pair n times at intervals of the order of T_2 . If the time-integrated FWM intensity does not increase with n , the measured value of T_2 is due mainly to chemical reactions.

References and Notes

- (1) Boyd, R. W.; Raymer, M. G.; Narum, P.; Harter, D. J. *Phys. Rev. A* **1981**, *24*, 411.
- (2) Friedmann, H.; Wilson-Gordon, A. D. *Phys. Rev. A* **1998**, *57*, 4854.
- (3) Allen, L.; Eberly, J. H. *Optical Resonance and Two-Level Atoms*; Wiley: New York, 1975.
- (4) Hioe, F. T. *Phys. Lett. A* **1983**, *99*, 150.
- (5) Oreg, J.; Hioe, F. T.; Eberly, J. H. *Phys. Rev. A* **1984**, *29*, 690.

- (6) Kuklinski, J. R.; Gaubatz, U.; Hioe, F. T.; Bergmann, K. *Phys. Rev. A* **1989**, *40*, 6741.
- (7) Shore, B. W. *Contemp. Phys.* **1995**, *36*, 15.
- (8) Vitanov, N. V.; Stenholm, S. *Phys. Rev. A* **1997**, *55*, 648; *Opt. Commun.* **1997**, *135*, 394.
- (9) Gaubatz, U.; Rudecki, P.; Schiemann, S.; Bergmann, K. *J. Chem. Phys.* **1990**, *92*, 5363.
- (10) Schiemann, S.; Kahn, A.; Steuerwald, S.; Bergmann, K. *Phys. Rev. Lett.* **1993**, *71*, 3637.
- (11) Lawall, J.; Prentiss, M. *Phys. Rev. Lett.* **1994**, *72*, 993.
- (12) Paspalakis, E.; Protopapas, E.; Knight, P. L. *Opt. Commun.* **1997**, *142*, 34.
- (13) Reference 3, eq 3.44.
- (14) Miklaszewski, W. *J. Opt. Soc. Am. B* **1995**, *12*, 1909.
- (15) Miklaszewski, W.; Fiutak, J. *Z. Phys. B* **1994**, *93*, 491.
- (16) Alhasan, A. M.; Fiutak, J.; Miklaszewski, W. *Z. Phys. B* **1992**, *88*, 349.
- (17) Ranka, J. K.; Shirmer, R. W.; Gaeta, A. *Phys. Rev. A* **1998**, *57*, R36.